

Hard X-ray emission in Centaurus A

B. RANI,^{1,2,3} S. A. MUNDO,⁴ R. MUSHOTZKY,⁴ A. Y. LIEN,⁵ M. A. GURWELL,⁶ AND J. Y. KIM^{7,8}

¹Korea Astronomy and Space science Institute, 776 Daedeokdae-ro, Yuseong-gu, Daejeon 30455, Korea

²University of Science and Technology, Korea, 217 Gajeong-ro, Yuseong-gu, Daejeon 34113, Korea

³Department of Physics, American University, Washington, DC 20016, USA

⁴Department of Astronomy, University of Maryland, College Park, MD 20742, USA

⁵University of Tampa, Department of Chemistry, Biochemistry, and Physics, 401 W. Kennedy Blvd, Tampa, FL 33606, USA

⁶Center for Astrophysics — Harvard & Smithsonian, 60 Garden Street, Cambridge, MA 02138 USA

⁷Department of Astronomy and Atmospheric Sciences, Kyungpook National University, Daegu 702-701, Republic Of Korea

⁸Max-Planck-Institut für Radioastronomie, Auf dem Hügel 69, D-53121 Bonn, Germany

ABSTRACT

We used 13 years of *Swift*/BAT observations to probe the nature and origin of hard X-ray (14-195 KeV) emission in Centaurus A. Since the beginning of the Swift operation in 2004, significant X-ray variability in the 14-195 KeV band is detected, with mild changes in the source spectrum. Spectral variations became more eminent after 2013, following a softer-when brighter trend. Using the power spectral density method, we found that the observed hard X-ray photon flux variations are consistent with a red-noise process of slope, -1.3 with no evidence for a break in the PSD. We found a significant correlation between hard X-ray and 230 GHz radio flux variations, with no time delay longer than 30 days. The temporal and spectral analysis rules out the ADAF (advection-dominated accretion flow) model, and confirms that the hard X-ray emission is produced in the inner regions of the radio jet.

Keywords: galaxies: active; galaxies: individual (Centarus A); X-rays: galaxies; radio continuum: galaxies

1. INTRODUCTION

The X-ray emitting sites in Active Galactic Nuclei (AGN) are not well understood. X-rays could either originate in the immediate vicinity of the central black hole (disk/corona) or further out in the jets. Some of these X-rays penetrate into the disk, where they are re-processed to produce the ‘*reflection*’ spectrum that includes the Fe K α line (Lohfink et al. 2013; Hinkle & Mushotzky 2021). The geometry of the disk/corona is an active area of research. A detailed understanding of disk/corona/jet contribution in the observed X-ray emission is a critical element in unraveling how the central engine of an AGN operates and feeds the jet. In this paper, we investigated the origin of hard X-ray emission in a nearby AGN, Centaurus A (Cen A hereafter), using the observed variations in the X-ray and radio regimes.

At a distance of $d \simeq 3.8$ Mpc (Harris et al. 2010), Cen A is the closest AGN hosting a supermassive black of $\sim 5 \times 10^7 M_{\odot}$ (Neumayer 2010). From the radio morphology of the lobes, Cen A is classified as Fanaroff-Riley type I (Fanaroff & Riley 1974). In fact, Cen A jet has been detected and extensively studied across the whole electromagnetic spectrum, radio to γ -rays (Wykes et al. 2015; Müller et al. 2014; Hardcastle et al.

2003; Worrall et al. 2008; Abdo et al. 2010; Janssen et al. 2021). In 2004, the source was first detected at TeV energies by H.E.S.S. (High Energy Stereoscopic System, Aharonian et al. 2009), and later by the Fermi/LAT at GeV energies (Abdo et al. 2010). Spatial extension of γ -ray emission is detected both at GeV (Abdo et al. 2010) and TeV energies (H. E. S. S. Collaboration et al. 2020), the physical origin of which remained unclear.

The X-ray (0.1-7 KeV) morphology of Cen A consists of a central bright AGN and a faint jet component surrounded by diffuse emission (Kraft et al. 2002). The source has a complex X-ray spectrum, comprising a soft (0.1-2 KeV) thermal plasma, a power-law continuum, and strong absorption of the power-law continuum. The location and structure of the absorbing material is still under debate (e.g. Evans et al. 2004; Markowitz et al. 2007; Fukazawa et al. 2011). The hard X-ray spectrum of the source can be well described by an absorbed power-law or thermal Comptonization spectrum with an Fe K α line, with no evidence for a high-energy exponential rollover (Fürst et al. 2016). Detection of a weak reflection component has been reported (Fukazawa et al. 2011; Burke et al. 2014), however, recent analysis has placed a very tight upper limit on the presence of a reflection component

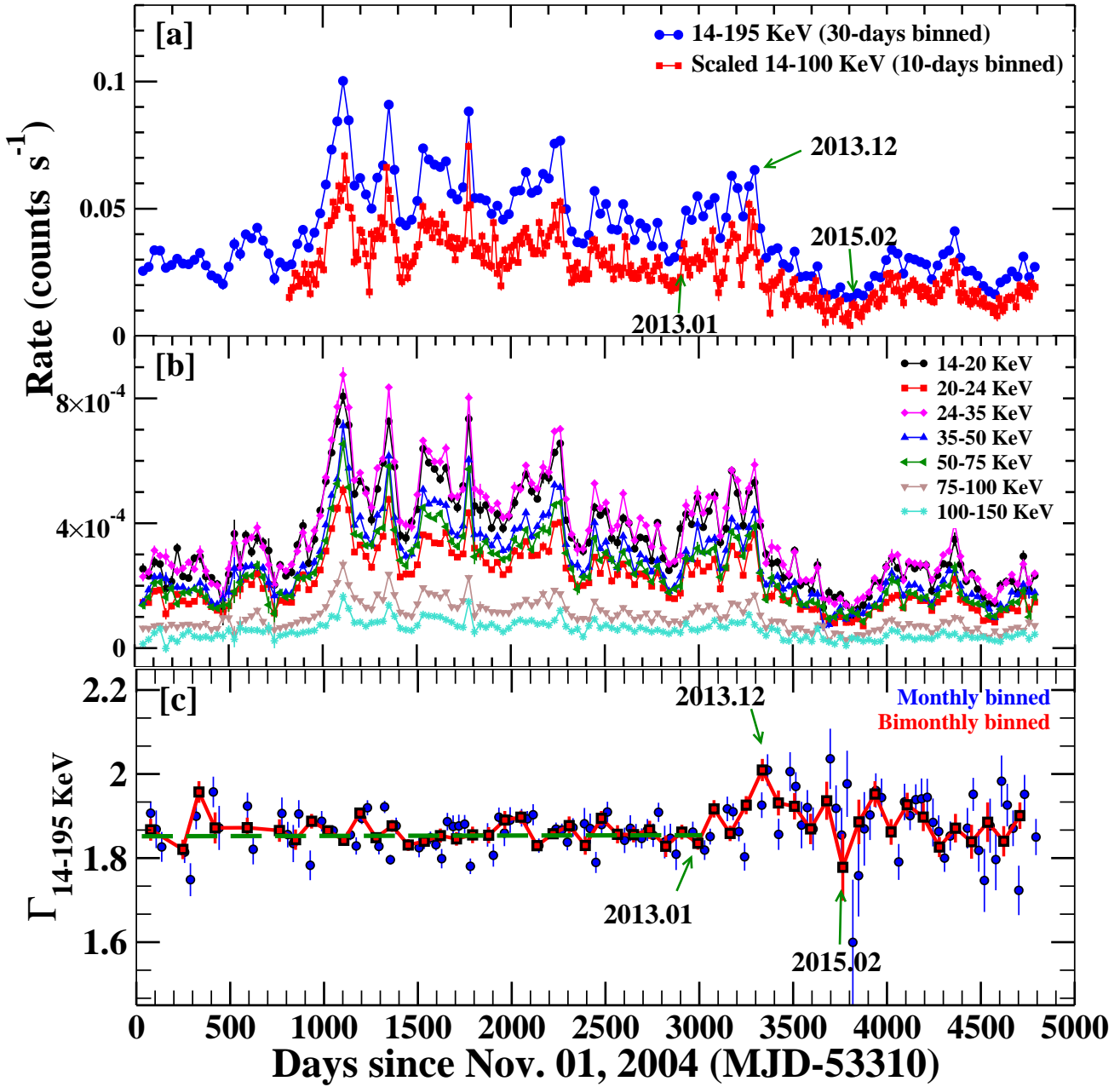


Figure 1. Photon flux and spectral variations observed in Cen A since November 2004: [a] Monthly averaged 14-195 KeV (blue circles) and 10-day binned 14-100 KeV (red squares) light curves. The 10-day binned data is scaled by a factor of 15, [b] Monthly averaged light curves in different energy bins, and [c] Hard X-ray photon index variations observed in the source. The green arrows mark the prominent spectral variability phases of the source (see Section 2.1 for more details).

(Beckmann et al. 2011; Fürst et al. 2016; Rothschild et al. 2011). Small changes in the hard X-ray power-law continuum photon index have been reported over the past decades (Baity et al. 1981; Rothschild et al. 2011; Fürst et al. 2016), with the slope being bounded between 1.6-1.85. This range of indices is consistent with what is found for Seyfert galaxies.

While the continuum flux is strongly variable over time, the flux of iron line remained stable, indicating a

strong variability of the equivalent width of the iron line (Rothschild et al. 2006). Even the joint spectral analysis using truly simultaneous *XMM-Newton* and *NuSTAR* data could not determine the physical origin of the hard X-ray emission in the source (Fürst et al. 2016). The study found no significant contribution from the hot interstellar medium (ISM), the outer jet and off-nuclear point sources, in the hard X-ray spectrum. Lack of reflection rules out the standard Seyfert-like geometry of the source of hard X-rays and reprocessing

material. Comptonization in an advection dominated accretion flow (ADAF) or at the base of the inner jet or a combination of the two were proposed as the possible mechanisms for the hard X-ray emission in the source (Fürst et al. 2016).

We present here a comprehensive analysis of the observed variations in X-ray and radio regions to better understand the nature and origin of the hard X-ray emission. The paper is structured as follows. In section 2, we present the data analysis and results. Results are discussed in Section 3, and summarized in Section 4.

2. DATA ANALYSIS AND RESULTS

2.1. X-rays

We investigated the X-ray flux and spectral variations of the source using data from the *Neil Gehrels Swift Observatory*/Burst Alert Telescope (*Swift*/BAT) 157-Month Hard X-ray Survey¹. While in survey mode (not specifically targeting a GRB), BAT continuously scans the sky with a time resolution as fine as 64 s (Krimm et al. 2013). Monthly averaged light curves and spectra of sources in the hard X-ray (14-195 KeV) sky are publicly available at <https://swift.gsfc.nasa.gov/results/bs157mon/671>. In addition to the 8-band (14-20, 20-24, 24-35, 35-50, 50-75, 75-100, 100-150, and 150-195 KeV) monthly averaged data, the website also provides 8-band snapshot light curves, starting from 2005. The snapshot light curves are extremely useful for exploring the short-timescale variability. The snapshot data is binned to generate 10-day binned light curves in different energy bands, then a total count rate for the 14-100 KeV energy range. While binning, we flagged the low-exposure (<1 day) epochs to reduce systematic errors. Given the low single-to-noise (S/N) ratio in bands 7 and 8, we discarded the 100-195 KeV energy band data.

Figure 1 (a) shows the monthly averaged hard X-ray (14-195 KeV) light curve from Dec. 2004 until Dec. 2017 (blue circles). Prominent flux variations were detected in the source during this period. The red squares show the 10-days binned light curves in the 14-100 KeV energy range. The count rates are scaled by a factor of 15 for visualization only. Given the high single-to-noise (S/N) ratio in the monthly binned data, the intensity variations can be studied in different energy bands. Photon flux light curves in different energy bands, 14-20, 20-24, 24-35, 35-50, 50-75, 75-100, and 100-150 KeV, are plotted in panel (b). Band 8 (150-195 KeV) is not included in the plot because of low S/N ratio. Similar variations are seen across the multiple bands. Variability is less pronounced at higher energy bands (>75 KeV) because of the low S/N ratio.

¹ <https://swift.gsfc.nasa.gov/results/bs157mon/671>

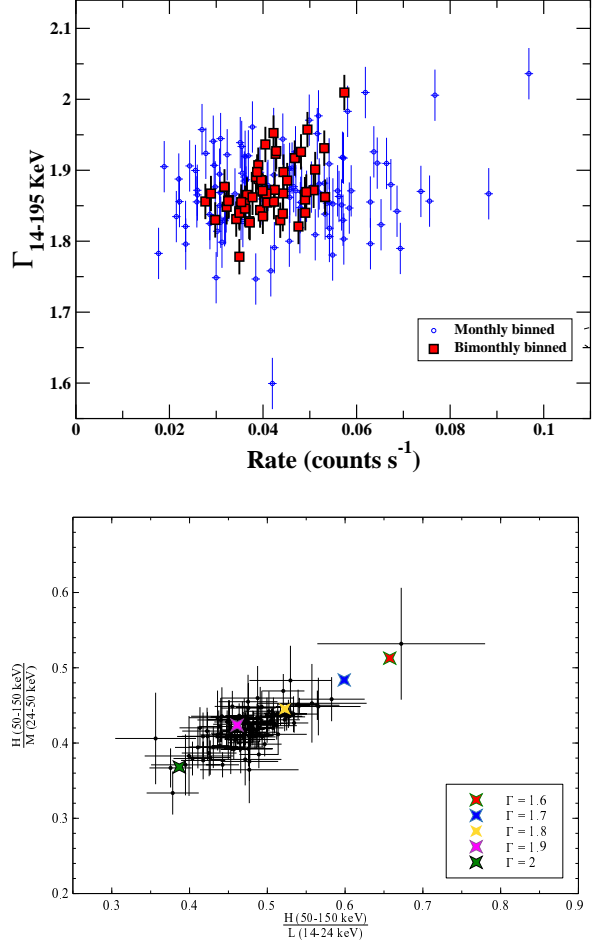


Figure 2. *Top:* Photon index versus photon flux plot. *Bottom:* Spectral variability of Cen A in the HR(hardness ratio)-plane. Black circles are the estimated hardness ratios in different energy channels, while the colored stars mark the simulated points.

Monthly (blue circles) and bimonthly (red squares) averaged hard X-ray photon index curve are illustrated in Fig. 1 (c). Despite significant flux variations in the X-ray bands, changes in the photon index were small but significant ($\Gamma \sim 1.7 - 1.9$) until the end of 2012. Spectral variations were more pronounced afterward. Steepening of the spectrum was observed until December 2013, reaching $\Gamma \sim 2.0$. Later, spectral hardening occurred until February 2015 ($\Gamma \sim 1.7$). The spectra soften back to the average value ($\Gamma \sim 1.8$) in recent years, with some mild variations. In short, the hard X-ray spectra follow a steeper-when-brighter trend. The trend is evident in index versus photon flux plot (Fig. 2 top). A linear Pearson correlation test is used to quantify the correlation; we obtained r_P (correlation coefficient) = 0.43 at the 99.8% confidence level for the bimonthly binned data, and $r_P = 0.16$ at the 90% confidence level for the monthly binned data.

We further investigate the spectral variability by analyzing hardness ratio (HR) time series. The monthly averaged data is used to calculate the time series in the following three

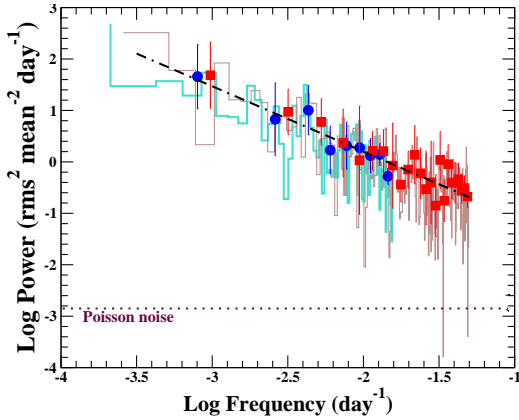


Figure 3. Raw PSD of the monthly (in cyan) and 10-day (in brown) binned X-ray light curves. The dotted line marks the estimated Poisson noise level. The blue circles and red squares are the logarithmically binned PSDs for the monthly and 10-day binned data sets, respectively. The black dashed line is the best fit power with a slope $= 1.27 \pm 0.13$.

energy bands: low or L-channel from 14–24 keV, medium or M-channel from 24–50 keV, and high or H-channel from 50–150 keV. We rebin the hard X-ray spectrum in this way in order to maximize the signal-to-noise. (We exclude the 150–195 keV data due to low S/N ratio.) We then calculate HR values using those three channels, and confirm through a chi-squared test that the HR time series show statistically significant variability ($p\text{-value} < 0.05$). Ratios of the time-series in different channels (HM versus HL) are then plotted against each other to produce an “HR-plane” (Fig. 2 black circles), and are used to investigate the nature of the spectral variability in the source. A visual correlation can be seen between the HL and ML ratios. Linear Pearson correlation analysis confirms the correlation between the two. Formally we get, the Pearson correlation coefficient equals to 0.71 at $>99.99\%$ confidence level. We further tested the spectral variations using simulations. The spectral simulations, using different power law slopes, were performed using the ‘*fakelit*’ command on Xspec (Arnaud 1996). The simulations were based on the simple “pegpwlw” model, with Γ in the range of 1 to 3 (typical photon indices of AGN in the *Swift*/BAT catalog). We then calculated the hardness ratios from the fake spectra (shown as colored stars in Fig. 2). The details of the simulations can be found in Mundo et al. 2022 (in preparation). The simulated points agree with the data, suggesting that the changing spectrum can be well described as a simple power-law with a varying photon index over monthly timescales, spanning the range 1.6–2.

The nature of hard X-ray variability in the source is explored using the power spectrum density (PSD Vaughan et al. 2003) analysis method. Both monthly averaged 14–195 KeV (data A) and 10-day binned 14–100 KeV (data B) light curves

are used for the PSD analysis. As a first step, we calculated the raw PSDs, squared modulus of the discrete Fourier transform. The raw PSDs are then logarithmically binned to extract the slope of the underlying power spectrum, $P(f) \propto f^\alpha$ (details are referred to Chidiac et al. 2016). The Poisson noise level in the PSD is calculated following Vaughan et al. (2003). The PSD analysis results are shown in Fig. 3, where cyan and brown steps are the raw PSDs respectively for data A and data B, blue circles and red squares are their logarithmic binned values; errors mark the scatter of the raw PSD points. The best-fit power-law slope for data A is $-(1.36 \pm 0.16)$, and for data B is $-(1.29 \pm 0.11)$. A combined power-law fit gives, $\alpha = -(1.27 \pm 0.13)$ (black dashed line in Fig. 3). We do not find any evidence of a break in the PSD, as is sometimes seen in the 2–10 KeV PSD of Seyfert galaxies (Vaughan et al. 2005). A similar value of the PSD slope was reported by Shimizu & Mushotzky (2013) using 58 months of the *Swift*/BAT data, and comparable slopes have been seen in PSDs of beamed AGN (Chidiac et al. 2016; Algaba et al. 2018) as well. This implies that the hard X-ray variability of the source can be characterized simply as a red-noise process. Since there is no excess power at any frequency in the given time range, the PSD analysis rules out the presence of periodic variations in the source.

2.2. Radio SMA

We used the 230 GHz data provided by the Submillimeter Array (SMA) Observer Center² database (Gurwell et al. 2007) to investigate the flux variations in the radio regime. Figure 4 (red squares) shows the flux density variations observed in the source since July 2005. The radio flux variations are superimposed on top of a constant flux level of about 6 Jy (dashed line), and this could be related to the extended jet emission (see Section 3.1 for details). Compared to X-rays (blue circles), the radio data is sparsely sampled, especially in the beginning (segment T1). Some similarities in the long-term decay trend can be seen in the two data sets over segment T2, and the flux variations are quite similar afterward (segment T3).

2.3. Cross-correlation

The apparent correlation among X-ray and radio data sets was quantified using the discrete correlation function (DCF Edelson & Krolik 1988) method, and the significance of the correlation was tested via simulations as discussed in Rani et al. (Section A 2014). The DCF results are presented in Fig. 4 (right). Monthly binned DCF points are in blue, while the red curves shows the 95% confidence levels. The DCF analysis of the two data sets shows a peak above 95%

² <http://sma1.sma.hawaii.edu/callist/callist.html>

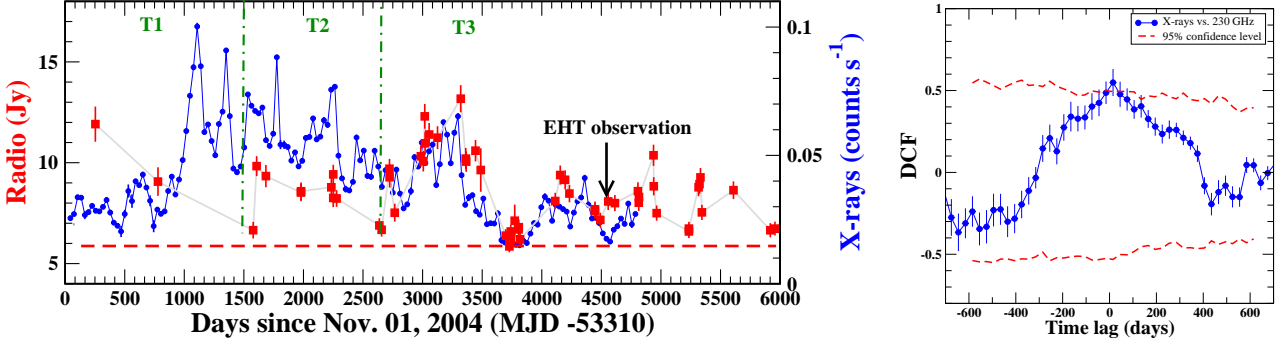


Figure 4. [Left] 230 GHz flux density light curve (red squares) superimposed on top of the 14-150 KeV light curve (blue circles). [Right] Cross-correlation analysis results: the DCF curve is in blue, while the red dashed-lines mark the 95% confidence level.

confidence level at 0 days. This implies that the flux variations at X-ray and regimes are well correlated with no time lag. Since the X-ray data is monthly sampled, a time-delay shorter than 30 days cannot be tested. The correlation analysis therefore suggests that the hard X-rays and radio emission regions are co-spatial. This agrees with a tight correlation found among the parsec-scale radio luminosity and X-ray luminosity of BAT detected Seyfert galaxies (Baek et al. 2019). Radio and X-ray (especially soft X-rays) correlations have also been reported in several other Seyfert galaxies (Chatterjee et al. 2009, 2011; Marscher et al. 2018) and explicitly used to probe the disk-jet connection in AGN.

3. DISCUSSION

Detailed spectral analysis (Fürst et al. 2016) suggests that the hard X-ray emitting site is close to the central engine, but could not disentangle the ADAF and jet contribution. The multi-wavelength variability analysis presented here allows us to do so. Using 13 years of Swift/BAT and 230 GHz data, we performed a detailed temporal and correlation analysis, which revealed the followings. Prominent flux variations were observed in the source since 2004, but spectral changes were rather moderate until 2012. Significant spectral variations were observed afterward, following a softer-when-brighter trend. The hard X-ray flux variability of the source is consistent with red-noise processes, with a slope ~ -1.3 . Variations in the hard X-ray and 230 GHz radio data are correlated, with no time lag. In the following subsections, we discuss the origin of hard X-ray emission in the context of ADAF and jet models.

3.1. Nature of X-ray variability

There have been many PSD studies of AGN, characterizing the PSD slopes, breaks, and their relation to the physical properties of the central engine. Breaks are a common feature in the PSDs of Seyfert galaxies (Papadakis 2004; Done & Gierliński 2005; Markowitz et al. 2003). These studies, however, are focused on the soft X-ray emission (<10 KeV), and the hard X-ray variability studies differ from

this picture (Shimizu & Mushotzky 2013). The hard X-ray PSD of Cen A is well-fitted using a slope of -1.3 , with no evidence of a break. If we scale the breaks seen in the X-ray PSDs by the mass as in McHardy et al. (2004), the predicted break timescale is higher than 20 days ($\log_{10}(\text{Frequency}) > -1.3 \text{ day}^{-1}$) and thus is not sensed by the BAT data. It is important to note that, unlike Seyfert galaxies, Cen A is a low-luminosity radio-loud AGN, and as our study suggests, the PSD slope is comparable to that has been seen in PSDs of beamed AGN.

Except for the power-law slope ($\Gamma = 1.6\text{--}2.0$), the X-ray spectrum of the source (no reflection and very high cutoff-Energy, Fürst et al. 2016) differs from that of Seyfert galaxies. Since the power-law slope from the jet and from the thermal Comptonization is very similar, the spectral slope cannot be used as a distinction between the two. However, the difference in source spectrum and temporal variations favor that the nature of X-ray emission in Cen A is similar to beamed AGN.

3.2. Nature of 230 GHz variability

The radio variations comprise of two components, quiescent and variable. As shown in Fig. 4, even at 230 GHz, we have about 6 Jy contribution from the extended jet region. Earlier studies found a contribution of about 7 Jy from the extended jet emission in the total flux density of the source (Israel et al. 2008). Since Cen A has a complex extended jet structure, the location of the variable component remained unclear. Using continuum observations in the millimeter and sub-millimeter regime, Israel et al. (2008) investigated the flux and spectral variability of the source, and reported that most (if not all) variations are from the milli-arcsecond core. On micro-arcsecond scales, the Event Horizon Telescope (EHT) discovered a completely different picture of the core (Janssen et al. 2021). The core of the source is opaque at 230 GHz and the turnover frequency is at $\sim\text{THz}$ frequencies. The source has a flux density of ~ 2 Jy with an edge-brightened jet. It is quite probable that either the flux density of the core or of the two lanes is varying, but multiple obser-

vations are required to confirm that. The radio luminosity of the source, measured by the EHT, is $7.5 \times 10^{39} \text{ erg s}^{-1}$. However, EHT observed the source not in its brightest phase (see Fig. 4). After subtracting the quiescent flux (6 Jy) from the total flux, the peak flux of the variable component is ~ 7 Jy, which corresponds to $2.6 \times 10^{40} \text{ erg s}^{-1}$.

3.3. ADAF versus jet models

In an ADAF model, the radio emission is because of cyclotron radiation from hot electrons in the equipartition magnetic field; it should be isotropic. In the absence of a radio jet, the expected radio luminosity is roughly proportional to the mass of the central black hole and its accretion rate (Yi & Boughn 1999; Mahadevan 1997), and is given by

$$L_{230 \text{ GHz}, \text{ADAF}} \sim 2.5 \times 10^{38} m_7^{8/5} \dot{m}_{-3}^{6/5} \text{ erg/s} \quad (1)$$

where m_7 is the black hole mass in units of $10^7 M_\odot$ and $\dot{m}_{-3} = \dot{m}/10^{-3}$, \dot{m} is accretion in units of Eddington rate. Using $m_7 = 5$ (Neumayer 2010) and $\dot{m}_{-3} = 0.2$ (Evans et al. 2004), the 230 GHz ADAF luminosity for Cen A is $\sim 5 \times 10^{38} \text{ erg s}^{-1}$, which is significantly lower than the observed 230 GHz radio luminosity. This implies that the ADAF component has a negligible contribution to the observed radio luminosity of the source.

Jet luminosity, in case of mainly powered by black hole accretion, can be estimated using eq. 9 in Janssen et al. (2021),

$$P_{\text{jet}} = 2.2 \times 10^{43} f(a_*) \left(\frac{\phi}{15} \right)^2 \left(\frac{\dot{M}}{10^{-6} \dot{M}_{\text{Edd}}} \right) \left(\frac{M}{6.2 \times 10^9 M_\odot} \right) \text{ erg s}^{-1}$$

where $0 \leq a_* \leq 1$ is the normalized black hole spin, $1 \leq \phi \leq 15$ is the normalized magnetic flux at the black hole event horizon, $f(a_*) \approx a_*^2 \left(1 + \sqrt{1 - a_*^2} \right)^{-2}$ (for $a_* < 0.95$), $\dot{M} = 2 \times 10^{-4} \dot{M}_{\text{Edd}}$, and $M = 5 \times 10^7 M_\odot$. For $a_* \leq 0.2$ and $\phi \leq 1$, we have a marginally low jet power of $P_{\text{jet}} \leq \times 10^{39} \text{ erg s}^{-1}$. Slightly larger values of $a_* = 0.3$ and $\phi = 2$ gives $P_{\text{jet}} \sim 1.5 \times 10^{40} \text{ erg s}^{-1}$, which well explains the observed radio luminosity.

Both ADAF and jet models predict a strong correlation between radio and X-ray flux variations. However, the ADAF models predict a very characteristic spectrum of slope 1/3 in the radio regime (Mahadevan 1997). The observed radio spectrum of the source has a slope of ~ 0.7 below the turnover frequency (around 5 to 20 GHz). A slightly steeper spectrum, slope 0.8, is observed at higher frequencies (Israel et al. 2008). This implies that the observed radio spectrum of the source is not consistent with the ADAF model. Moreover, the shape of the hard X-ray spectrum in

ADAF models is thermal bremsstrahlung not a power-law. For low luminosity AGN (accreting close to $\dot{m}_{\text{critical}} = 0.003$ to 0.02, Mahadevan 1997; Narayan 1996), X-ray spectrum is very hard ($\Gamma \sim 0.7$). The power-law spectrum of Cen A, Γ varying between 1.7 to 2, rules out the ADAF models. Another factor that argues in favor of the jet-based origin of the hard X-ray emission is the steeping of the X-ray spectrum as the source gets brighter. ADAF models predict harder-when-brighter behavior (Esin et al. 1997). As discussed in Section 2.1, the spectrum gets steeper while the source gets brighter.

4. CONCLUSIONS

We present a thorough analysis of hard X-ray emission from Cen A using 13 years (Dec. 2004–Dec. 2017) of *Swift*/BAT observations. Prominent photon flux variations were detected during this period, and the variations are consistent with a red-noise process of slope -1.3 . The source spectral variations were rather moderate until the end of 2012; a steeper-while-brighter trend was observed afterward. We found a significant correlation between the hard X-ray and 230 GHz flux variations with no time-lag, indicating a co-spatiality of their emitting sites.

Previous spectral analysis confirms that hard X-ray emission of the source is confined within the core, and is produced either via Comptonization in an ADAF flow or at the base of the inner jet (Fürst et al. 2016). The study could not disentangle the two. However, variability analysis and the broadband spectral energy distribution studies of the source, using decade long *Rossi X-ray Timing Explorer* (RXTE) observations, favored the jet based origin of the hard X-ray emission (Rothschild et al. 2011). Using a comprehensive analysis of the hard X-ray emission and its correlation with the 230 GHz observations, we probe the hard X-ray emitting site in Cen A. The following arguments rule out the ADAF models: (1) observed 230 GHz luminosity is significantly higher than $L_{230 \text{ GHz}, \text{ADAF}}$, (2) radio spectral slope (~ 0.7 – 0.8) contradicts with the characteristic slope of 1/3 predicted by the ADAF models, (3) power-law X-ray spectral shape, and (4) a softer-when brighter behavior of the hard X-ray spectra. The study confirms the jet-based origin of the hard X-ray emission in the source.

- 1 BR acknowledges support from the National Research Founda-
- 2 tion of Korea (grant number 2021R1A2C1095799). JYK
- 3 acknowledges support from the National Research Founda-
- 4 tion of Korea (grant number 2022R1C1C1005255). The Sub-
- 5 millimeter Array is a joint project between the Smithsonian
- 6 Astrophysical Observatory and the Academia Sinica Institute
- 7 of Astronomy and Astrophysics and is funded by the Smith-
- 8 sonian Institution and the Academia Sinica. We thank the
- 9 reviewer for an insightful review of the paper.

REFERENCES

- Abdo, A. A., Ackermann, M., Ajello, M., et al. 2010, *Science*, 328, 725, doi: [10.1126/science.1184656](https://doi.org/10.1126/science.1184656)
- Aharonian, F., Akhperjanian, A. G., Anton, G., et al. 2009, *ApJL*, 695, L40, doi: [10.1088/0004-637X/695/1/L40](https://doi.org/10.1088/0004-637X/695/1/L40)
- Algaba, J.-C., Lee, S.-S., Kim, D.-W., et al. 2018, *ApJ*, 852, 30, doi: [10.3847/1538-4357/aa9e50](https://doi.org/10.3847/1538-4357/aa9e50)
- Arnaud, K. A. 1996, in *Astronomical Society of the Pacific Conference Series*, Vol. 101, *Astronomical Data Analysis Software and Systems V*, ed. G. H. Jacoby & J. Barnes, 17
- Baek, J., Chung, A., Schawinski, K., et al. 2019, *MNRAS*, 488, 4317, doi: [10.1093/mnras/stz1995](https://doi.org/10.1093/mnras/stz1995)
- Baity, W. A., Rothschild, R. E., Lingenfelter, R. E., et al. 1981, *ApJ*, 244, 429, doi: [10.1086/158719](https://doi.org/10.1086/158719)
- Beckmann, V., Jean, P., Lubiński, P., Soldi, S., & Terrier, R. 2011, *A&A*, 531, A70, doi: [10.1051/0004-6361/201016020](https://doi.org/10.1051/0004-6361/201016020)
- Burke, M. J., Jourdain, E., Roques, J.-P., & Evans, D. A. 2014, *ApJ*, 787, 50, doi: [10.1088/0004-637X/787/1/50](https://doi.org/10.1088/0004-637X/787/1/50)
- Chatterjee, R., Marscher, A. P., Jorstad, S. G., et al. 2009, *ApJ*, 704, 1689, doi: [10.1088/0004-637X/704/2/1689](https://doi.org/10.1088/0004-637X/704/2/1689)
- . 2011, *ApJ*, 734, 43, doi: [10.1088/0004-637X/734/1/43](https://doi.org/10.1088/0004-637X/734/1/43)
- Chidiac, C., Rani, B., Krichbaum, T. P., et al. 2016, *A&A*, 590, A61, doi: [10.1051/0004-6361/201628347](https://doi.org/10.1051/0004-6361/201628347)
- Done, C., & Gierliński, M. 2005, *MNRAS*, 364, 208, doi: [10.1111/j.1365-2966.2005.09555.x](https://doi.org/10.1111/j.1365-2966.2005.09555.x)
- Edelson, R. A., & Krolik, J. H. 1988, *ApJ*, 333, 646, doi: [10.1086/166773](https://doi.org/10.1086/166773)
- Esin, A. A., McClintock, J. E., & Narayan, R. 1997, *ApJ*, 489, 865, doi: [10.1086/304829](https://doi.org/10.1086/304829)
- Evans, D. A., Kraft, R. P., Worrall, D. M., et al. 2004, *ApJ*, 612, 786, doi: [10.1086/422806](https://doi.org/10.1086/422806)
- Fanaroff, B. L., & Riley, J. M. 1974, *MNRAS*, 167, 31P, doi: [10.1093/mnras/167.1.31P](https://doi.org/10.1093/mnras/167.1.31P)
- Fukazawa, Y., Hiragi, K., Yamazaki, S., et al. 2011, *ApJ*, 743, 124, doi: [10.1088/0004-637X/743/2/124](https://doi.org/10.1088/0004-637X/743/2/124)
- Fürst, F., Müller, C., Madsen, K. K., et al. 2016, *ApJ*, 819, 150, doi: [10.3847/0004-637X/819/2/150](https://doi.org/10.3847/0004-637X/819/2/150)
- Gurwell, M. A., Peck, A. B., Hostler, S. R., Darrah, M. R., & Katz, C. A. 2007, in *Astronomical Society of the Pacific Conference Series*, Vol. 375, *From Z-Machines to ALMA: (Sub)Millimeter Spectroscopy of Galaxies*, ed. A. J. Baker, J. Glenn, A. I. Harris, J. G. Mangum, & M. S. Yun, 234
- H. E. S. S. Collaboration, Abdalla, H., Adam, R., et al. 2020, *Nature*, 582, 356, doi: [10.1038/s41586-020-2354-1](https://doi.org/10.1038/s41586-020-2354-1)
- Hardcastle, M. J., Worrall, D. M., Kraft, R. P., et al. 2003, *ApJ*, 593, 169, doi: [10.1086/376519](https://doi.org/10.1086/376519)
- Harris, G. L. H., Rejkuba, M., & Harris, W. E. 2010, *PASA*, 27, 457, doi: [10.1071/AS09061](https://doi.org/10.1071/AS09061)
- Hinkle, J. T., & Mushotzky, R. 2021, *MNRAS*, 506, 4960, doi: [10.1093/mnras/stab1976](https://doi.org/10.1093/mnras/stab1976)
- Israel, F. P., Raban, D., Booth, R. S., & Rantakyö, F. T. 2008, *A&A*, 483, 741, doi: [10.1051/0004-6361:20079229](https://doi.org/10.1051/0004-6361:20079229)
- Janssen, M., Falcke, H., Kadler, M., et al. 2021, *Nature Astronomy*, 5, 1017, doi: [10.1038/s41550-021-01417-w](https://doi.org/10.1038/s41550-021-01417-w)
- Kraft, R. P., Forman, W. R., Jones, C., et al. 2002, *ApJ*, 569, 54, doi: [10.1086/339062](https://doi.org/10.1086/339062)
- Krimm, H. A., Holland, S. T., Corbet, R. H. D., et al. 2013, *ApJS*, 209, 14, doi: [10.1088/0067-0049/209/1/14](https://doi.org/10.1088/0067-0049/209/1/14)
- Lohfink, A. M., Reynolds, C. S., Jorstad, S. G., et al. 2013, *ApJ*, 772, 83, doi: [10.1088/0004-637X/772/2/83](https://doi.org/10.1088/0004-637X/772/2/83)
- Mahadevan, R. 1997, *ApJ*, 477, 585, doi: [10.1086/303727](https://doi.org/10.1086/303727)
- Markowitz, A., Edelson, R., Vaughan, S., et al. 2003, *ApJ*, 593, 96, doi: [10.1086/375330](https://doi.org/10.1086/375330)
- Markowitz, A., Takahashi, T., Watanabe, S., et al. 2007, *ApJ*, 665, 209, doi: [10.1086/519271](https://doi.org/10.1086/519271)
- Marscher, A. P., Jorstad, S. G., Williamson, K. E., et al. 2018, *ApJ*, 867, 128, doi: [10.3847/1538-4357/aae4de](https://doi.org/10.3847/1538-4357/aae4de)
- McHardy, I. M., Papadakis, I. E., Uttley, P., Page, M. J., & Mason, K. O. 2004, *MNRAS*, 348, 783, doi: [10.1111/j.1365-2966.2004.07376.x](https://doi.org/10.1111/j.1365-2966.2004.07376.x)
- Müller, C., Kadler, M., Ojha, R., et al. 2014, *A&A*, 569, A115, doi: [10.1051/0004-6361/201423948](https://doi.org/10.1051/0004-6361/201423948)
- Mundo, et al. 2022 (in preparation)
- Narayan, R. 1996, *ApJ*, 462, 136, doi: [10.1086/177136](https://doi.org/10.1086/177136)
- Neumayer, N. 2010, *PASA*, 27, 449, doi: [10.1071/AS09080](https://doi.org/10.1071/AS09080)
- Papadakis, I. E. 2004, *MNRAS*, 348, 207, doi: [10.1111/j.1365-2966.2004.07351.x](https://doi.org/10.1111/j.1365-2966.2004.07351.x)
- Rani, B., Krichbaum, T. P., Marscher, A. P., et al. 2014, *A&A*, 571, L2, doi: [10.1051/0004-6361/201424796](https://doi.org/10.1051/0004-6361/201424796)
- Rothschild, R. E., Markowitz, A., Rivers, E., et al. 2011, *ApJ*, 733, 23, doi: [10.1088/0004-637X/733/1/23](https://doi.org/10.1088/0004-637X/733/1/23)
- Rothschild, R. E., Wilms, J., Tomsick, J., et al. 2006, *ApJ*, 641, 801, doi: [10.1086/500534](https://doi.org/10.1086/500534)
- Shimizu, T. T., & Mushotzky, R. F. 2013, *ApJ*, 770, 60, doi: [10.1088/0004-637X/770/1/60](https://doi.org/10.1088/0004-637X/770/1/60)
- Vaughan, S., Edelson, R., Warwick, R. S., & Uttley, P. 2003, *MNRAS*, 345, 1271, doi: [10.1046/j.1365-2966.2003.07042.x](https://doi.org/10.1046/j.1365-2966.2003.07042.x)
- Vaughan, S., Fabian, A. C., & Iwasawa, K. 2005, *Ap&SS*, 300, 119, doi: [10.1007/s10509-005-1211-x](https://doi.org/10.1007/s10509-005-1211-x)
- Worrall, D. M., Birkinshaw, M., Kraft, R. P., et al. 2008, *ApJL*, 673, L135, doi: [10.1086/528681](https://doi.org/10.1086/528681)
- Wykes, S., Hardcastle, M. J., & Croston, J. H. 2015, *MNRAS*, 454, 3277, doi: [10.1093/mnras/stv2187](https://doi.org/10.1093/mnras/stv2187)
- Yi, I., & Boughn, S. P. 1999, *ApJ*, 515, 576, doi: [10.1086/307041](https://doi.org/10.1086/307041)